Discovery Potential for New Phenomena*

Stephen Godfrey[1], JoAnne L. Hewett[2], and Lawrence E. Price[3]
[1]*Ottawa Carleton Institute for Physics, Carleton University, Ottawa, Canada*
[2]*Stanford Linear Accelerator Center, Stanford, CA 94309, USA*
[3]*High Energy Physics Division, Argonne National Laboratory, Argonne, IL 60439, USA*

Working Group Members: J. Appel (FNAL), P. de Barbaro (Rochester), M. Berger† (Indiana), G. Burdman (Wisconsin), K. Cheung† (Texas), F. Cuypers (PSI), S. Davidson (Max Planck), M. Doncheski (Penn State - Mont Alto), E. Eichten (FNAL), C. Greub (DESY), R. Harris† (FNAL), X.-G. He (Melbourne), C. Heusch (U.C. Santa Cruz), H. Kagan† (Ohio State), P. Kalyniak (Carleton), D. Krakauer† (ANL), K. Kumar (Princeton), T. Lee (FNAL), J. Lykken (FNAL), K. Maeshima† (FNAL), I. Melo (Carleton), W. Merritt† (FNAL), P. Minkowski (PSI), R. Peccei (UCLA), S. Riemann (Zeuthen), T. Rizzo† (SLAC), J. Rowe (U.C. Davis), D. Silverman (U.C. Irvine), E. Simmons (Boston), J. Slaughter (FNAL), M. Swartz† (SLAC), D. Toback (Chicago), R. Vidal (FNAL), J. Womersley (FNAL), G. Wrochna (CERN), J. Wudka (U.C. Riverside), C.-E. Wulz (Austria, OAW)

Abstract

We examine the ability of future facilities to discover and interpret non-supersymmetric new phenomena. We first explore explicit manifestations of new physics, including extended gauge sectors, leptoquarks, exotic fermions, and technicolor models. We then take a more general approach where new physics only reveals itself through the existence of effective interactions at lower energy scales.

Summary Report of the New Phenomena Working Group. To appear in the *Proceedings of the 1996 DPF/DPB Summer Study on New Directions for High Energy Physics - Snowmass96*, Snowmass, CO, 25 June - 12 July 1996.

* Work supported by the U.S. Department of Energy under contracts DE-AC03-76SF00515 and W-31-109-ENG-38, and the Natural Sciences and Engineering Research Council of Canada
† Subgroup Convener

Stephen Godfrey[1], JoAnne L. Hewett[2], and Lawrence E. Price[3]
[1]*Ottawa Carleton Institute for Physics, Carleton University, Ottawa, Canada*
[2]*Stanford Linear Accelerator Center, Stanford, CA 94309, USA*
[3]*High Energy Physics Division, Argonne National Laboratory, Argonne, IL 60439, USA*

Working Group Members(† Subgroup Convener): J. Appel (FNAL), P. de Barbaro (Rochester), M. Berger† (Indiana), G. Burdman (Wisconsin), K. Cheung† (Texas), F. Cuypers (PSI), S. Davidson (Max Planck), M. Doncheski (Penn State - Mont Alto), E. Eichten (FNAL), C. Greub (DESY), R. Harris† (FNAL), X.-G. He (Melbourne), C. Heusch (U.C. Santa Cruz), H. Kagan† (Ohio State), P. Kalyniak (Carleton), D. Krakauer† (ANL), K. Kumar (Princeton), T. Lee (FNAL), J. Lykken (FNAL), K. Maeshima† (FNAL), I. Melo (Carleton), W. Merritt† (FNAL), P. Minkowski (PSI), R. Peccei (UCLA), S. Riemann (Zeuthen), T. Rizzo† (SLAC), J. Rowe (U.C. Davis), D. Silverman (U.C. Irvine), E. Simmons (Boston), J. Slaughter (FNAL), M. Swartz† (SLAC), D. Toback (Chicago), R. Vidal (FNAL), J. Womersley (FNAL), G. Wrochna (CERN), J. Wudka (U.C. Riverside), C.-E. Wulz (Austria, OAW)

ABSTRACT

We examine the ability of future facilities to discover and interpret non-supersymmetric new phenomena. We first explore explicit manifestations of new physics, including extended gauge sectors, leptoquarks, exotic fermions, and technicolor models. We then take a more general approach where new physics only reveals itself through the existence of effective interactions at lower energy scales.

I. INTRODUCTION

Although the Standard Model (SM) of particle physics is in complete agreement with present experimental data, it is believed to leave many questions unanswered and this belief has resulted in numerous attempts to discover a more fundamental underlying theory. In planning for the future, it is reasonable to consider what classes of new interactions might exist and what types of facilities would be best to first discover them and then to elucidate their properties. In fact, numerous types of experiments may expose the existence of new physics; here we focus on the potential signatures at high energy colliders.

History shows us that the most exciting discoveries are those that are unexpected. Unfortunately, it is difficult to concretely plan for the unexpected. The best we can do is to examine the discovery capabilities of future facilities for a wide variety of anticipated particles under the hope that they will be sufficient in uncovering the truth in nature. To accomplish this task, the 1996 Snowmass working group on new phenomena decided to construct a physics matrix, where numerous new physics possibilities were investigated at various collider options. The accelerators used for our physics studies were those defined by the Snowmass organizing committee. The new phenomena scenarios were divided into three main categories: (i) New Gauge Bosons, (ii) New Particles, and (iii) New Interactions. The remainder of this report presents the conclusions from each category. We note that our physics matrix is strikingly similar to that presented in the Proceedings of the 1982 Snowmass Summer Study[1], both in physics topics and colliders. It is disappointing that so little progress has been made in our attempt to understand the fundamental theory of nature.

Before turning to our investigations of searches for new phenomena at high energy colliders, we note that virtual effects of new physics also provides an important opportunity to probe the presence of new interactions[2]. This complementary approach examines the indirect effects of new physics in higher order processes by testing for deviations from SM predictions. In this case, one probes (i) the radiative corrections to perturbatively calculable processes, as well as (ii) transitions which are either suppressed or forbidden in the SM. Both of these scenarios carry the advantage of being able to explore the presence of new physics at very high mass scales. In some cases the constraints obtained in this manner surpass those from collider searches, with a recent example being given by the strong bounds on the mass of a charged Higgs boson from the decay $B \to X_s\gamma$[3]. In other cases, entire classes of models are found to be incompatible with the data. Given the large amount of high luminosity 'low-energy' data which is presently available and will continue to accumulate during the next decade, the loop effects of new interactions in rare processes and precision measurements will play a major role in the search for physics beyond the SM.

It is well-known that physics outside of the SM is required in order to obtain unification of the strong and electroweak forces. Unification attempts using only the SM particle content fail because they predict too small a value of the unification scale, implying a rapidly decaying proton, as well as leading to values of $\alpha_s(M_Z)$ which are significantly smaller than the experimentally determined value by many standard deviations. The oft-quoted remedy to this situation is to introduce supersymmetry at the TeV scale[4, 5]. In fact, the introduction of the minimal supersymmetric particle content modifies the evolution of the coupling constants such that unification is obtained at a higher scale and there is agreement with present data. The most frequently considered case is where supersymmetry (SUSY) is embedded into a SUSY $SU(5)$ Grand Unified Theory (GUT). However, satisfactory unification is also achieved in larger SUSY GUTs, such as supersymmetric $SO(10)$ and E_6. In these cases both the gauge sector and particle content are enlarged, leading to the many possible types of new phenomena which are discussed in the first two sections of this report. In particular, it has been shown[6] that successful unification is achievable in SUSY $SO(10)$ with a light right-handed mass scale, resulting (amongst other things) in a right-handed

possible for non-supersymmetric models with additional particle content to show similar unification properties[5, 7], although such cases are difficult to arrange. One such scenario is that where the SM particle content is augmented by a weak iso-doublet of leptoquarks ($\widetilde{R}_{2L}$, to be defined below) and an additional Higgs doublet. The two-loop renormalization group analysis of this case[8] is presented in Fig. 1. Here, one obtains the value $\alpha_s(M_Z) = 0.123$ and a proton lifetime of $10^{32\pm1}$ years consistent with experiment.

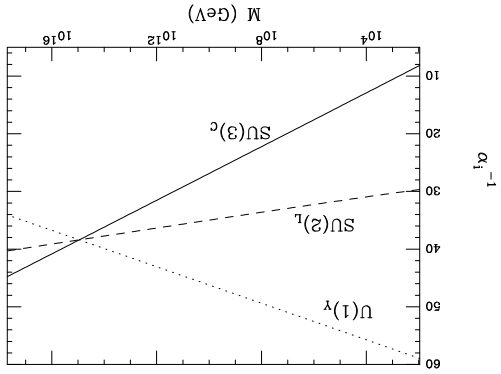

Figure 1: Two-loop Renormalization Group Evolution of the coupling constants in the scenario where the SM particle content is augmented by a pair of leptoquarks and an additional Higgs doublet. (From Ref. [8].)

II. NEW GAUGE BOSONS

New gauge bosons (NGBs) are a feature of many extensions of the standard model such as grand unified theories, Left-Right symmetric models, supersymmetric models, and superstring theories. If a Z' or W' were discovered it would have important implications for what lies beyond the standard model. It is therefore important to study and compare what the next generation of colliders can tell us about NGBs. There is a vast literature on the subject of discovery and identification of NGBs [9]. The NGB subgroup goals were to extend previous studies in several directions:

1. To extend the existing analysis to the colliders included as part of the Snowmass study that have not been previously studied.

2. To extend studies to include gauge bosons that have received incomplete attention in the past, in particular discovery reaches for W' bosons at e^+e^- colliders.

3. To redo earlier studies including important considerations so far neglected. For example, the cross sections for Z' and W''s at hadron colliders have almost always been calculated in the narrow width approximation, generally decaying only to standard model fermions, and not including signal may broaden sufficiently that it is overwhelmed by background. At the minimum, it is important to know how these contributions will effect the discovery limits.

In this report we summarize the results of these studies and attempt to integrate them with previous results to present a complete overview of the subject of NGBs. By necessity this summary will omit important details of the various calculations. We therefore direct the interested reader to the more complete and detailed subgroup summary by Rizzo [10] and the individual contributed reports to the proceedings.

A. Introduction to Models

Quite a few models predicting NGBs exist in the literature. These can be divided into two broad classes depending on whether or not they originate from a GUT group such as $SO(10)$ or E_6. We focus our studies on a few representative models, which although far from exhaustive, form a representative set for the purposes of this study. To be specific the models we consider are:

1. The E_6 effective rank-5 model (ER5M) which predicts a Z' whose couplings depend on a parameter $-\pi/2 \leq \theta_{E_6} \leq \pi/2$. Models ψ ($\theta_{E_6} = 0$), χ ($\theta_{E_6} = -\pi/2$), I ($\theta_{E_6} = -\cos^{-1}\sqrt{3/8}$), and η ($\theta_{E_6} = \cos^{-1}\sqrt{5/8}$) denote common cases discussed in the literature.

2. The Sequential Standard Model (SSM) where the new W' and Z' are just heavy versions of the SM. This is not a true model but is often used as benchmark by experimenters.

3. The Un-Unified Model (UUM) based on the group $SU(2)_\ell \times SU(2)_q \times U(1)_Y$, which has a single free parameter $0.24 \leq s_\phi \leq 0.99$

4. The Left-Right Symmetric Model (LRM) based on the group $SU(2)_L \times SU(2)_R \times U(1)_{B-L}$ which has a free parameter $\kappa = g_R/g_L \geq 0.55$ which is just the ratio of the gauge couplings.

5. The Alternative Left-Right Model (ALRM) based on the same extended group as the LRM but now arising from E_6 where the fermion assignments are different from those in the LRM due to an ambiguity in how they are embedded in the **27** representation.

Details of these models and complete references are given in Ref. [9].

Although searches for NGBs, and indeed any new particles, are of interest on general grounds, if there are theoretical motivations for them to be accessible at existing or future colliders their phenomenological interest is enhanced considerably. In a contribution to these proceedings, Lykken [11] examined this issue for the case of a new $U(1)'$ gauge group in the general context of SUSY-GUTS and String Theory with weak-scale supersymmetry. He found that a broad class of models predict a Z' boson whose mass is in the range $250\,\mathrm{GeV} - 2\,\mathrm{TeV}$. However, these models require either discrete tuning of the $U(1)'$ charges or a leptophobic Z'.

Two distinct search strategies exist for extra gauge bosons. Indirect evidence for gauge bosons, where deviations from the standard model would signal new physics, are the primary approach at e^+e^-, e^-e^-, $\mu^+\mu^-$, and ep colliders while direct evidence signalled but clusters of high invariant mass lepton pairs is the primary strategy employed at hadron colliders. A large literature exists on search strategies for extra gauge bosons and their discovery limits, for existing and proposed high energy colliders.

1. *Hadron Colliders*

In hadron colliders NGBs will generally reveal themselves through decays to charged lepton pairs for Z' bosons and to charged leptons plus missing E_T for W' bosons. There are exceptions such as leptophobic Z' bosons decay to quark pairs which would be observed as bumps in dijet invariant mass distributions [12].

Search limits have been obtained previously for all the hadron colliders [13] considered at Snowmass with the exception of the 200 TeV (PIPETRON) collider. However, these results were generally obtained using the narrow width approximation with the NGB decaying only to conventional fermions and with possible corrections to account for detector acceptances and efficiencies. Discovery was defined to be 10 dilepton signal events. Detailed detector simulations for the the Tevatron and LHC validated this approximation as a good estimator of the true search reach. The discovery reaches for hadron colliders are summarized in Table I [14]. TeV33 will, for the first time allow us to approach the 1 TeV mass scale for Z' bosons. For the 60 and 200 TeV machines the higher $q\bar{q}$ luminosities in the $p\bar{p}$ mode leads to significantly greater ($\simeq 30-50\%$) search reach. It is important to note that in many models the Z' can also decay to exotic fermions and/or SUSY particles which will reduce B_ℓ and thus the search reach (about 10% reduction in search reach for a factor of 2 decrease in B_ℓ) [14, 15].

Wulz performed detailed Monte Carlo studies of Z' discovery limits for the LHC at $\sqrt{s} = 14$ TeV using the CMS detector simulation and PYTHIA to generate the Z' events [16]. Exotic fermions were not assumed. Drell-Yan and Z backgrounds were taken into account and were approximately two orders of magnitude below the signal. Heavy flavor backgrounds from $t\bar{t}$ and $b\bar{b}$ are completely negligible. Figure 2 shows reconstructed invariant mass spectra for $M_{Z'} = 5$ TeV and an integrated luminosity of 100 fb^{-1}. The discovery limits obtained by Wulz are consistent with the numbers given in Table I.

Unlike the Z' case, W_R searches have many subtleties. Typically, search limits are obtained by assuming (i) the $q'\bar{q}W_R$ production vertex has SM strength, (ii) $\kappa = 1$, (iii) $|V_{L_{ij}}| = |V_{R_{ij}}|$ (the CKM mixing matrix $V_R \equiv V_L$), and (iv) $B(W_R \to \ell\nu)$ is given by the decay to SM fermions. If assumption (ii) is invalid large search reach degradations are possible, especially at $p\bar{p}$ colliders, due to modification of the parton luminosities [14]. Again, the search reaches are higher ($\sim 25\%$) in the case of $p\bar{p}$.

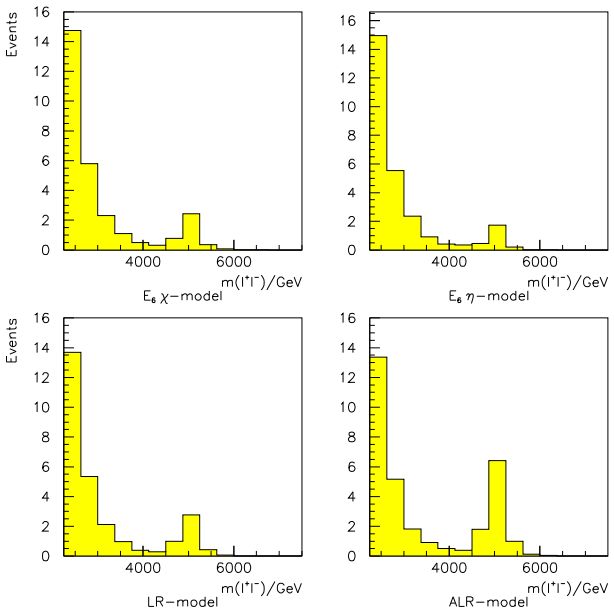

Figure 2: Invariant mass spectra for four Z' models with $M_{Z'} = 5$ TeV. (From Ref. [16].)

2. *Lepton Colliders*

If Z''s and W''s are to be found at lepton colliders their existence is most likely to be revealed through deviations from SM predictions. To represent a meaningful signal of new physics deviations should be observed in as many observables as possible. Typically observables are constructed from cross sections to specific fermions in the final state; cross sections, σ^f, forward-backward asymmetries, A^f_{FB}, and left-right polarization asymmetries, A^f_{LR}, where $f = \mu$, τ, c, b, and had =sum over hadrons. Expressions for these observables are included in the contribution of Godfrey [17]. The report by Godfrey gives discovery limits for high energy e^+e^- and $\mu^+\mu^-$ colliders. The main distinction between the two types of colliders is that e^+e^- colliders should have high polarizations while $\mu^+\mu^-$ colliders are not expected to. That analysis assumed 90% electron polarization (for the e^+e^- case), 35% c-tagging efficiency and 60% b-tagging efficiency. In retrospect these efficiencies are likely to be overly optimistic for the $\mu^+\mu^-$ collider. Rizzo performed a similar analysis except for the e^+e^- colliders he included t-quark final states and the additional complications of angular cuts and initial state radiation(ISR) [14]. He found that ISR reduces the search reach by 15-20% while beam polarization increases the reach by 15-80%, depending on the specific model and the machine energy.

In principle the NLC can be run in a polarized e^-e^- mode with luminosity and polarization comparable to the e^+e^- mode. Since both e^- beams are polarized the effective polarization is larger and, due to the large Moller cross section there is significant sensitivity to the existence of a Z'. Cuypers studied the sensitivity of $e^+e^- \to \mu^+\mu^-$, $e^+e^- \to e^+e^-$ and $e^-e^- \to e^-e^-$

rors due to imperfect polarization measurement, finite detector acceptance, and luminosity uncertainties [18]. In general the e^-e^- reach is slightly superior to that obtained in the e^+e^- mode when only the leptonic final states are used. However, Rizzo found that once one includes the additional information from the quark sector the e^+e^- mode offers a higher reach [14].

There has been very little work done on searches for W' at e^+e^- colliders. In a contribution to the proceedings Hewett [20] studied the sensitivity of the reaction $e^+e^- \to \nu\bar{\nu}\gamma$ to W' bosons which would contribute via t-channel exchange. She found that the resulting photon energy spectrum would be sensitive to a W_R mass of at most $2\times\sqrt{s}$ in the LRM and in the UUM the W_H discovery reach barely extends above $\sqrt{s}$ for small values of $\sin\phi$. However for larger values of $\sin\phi$ the reach grows to several times $\sqrt{s}$ due to the increase in leptonic couplings for $\sin\phi > 0.5$. Although these preliminary results do not directly compete with the discovery reach at the LHC they do demonstrate that it is possible to observe the effects of W' bosons with masses greater than $\sqrt{s}$ at e^+e^- colliders.

C. Coupling Determination

If evidence for NGBs were found the next task would be to obtain information that would verify the discovery and could determine the nature of the NGB. Both hadron and lepton colliders can play complementary roles in this task, each having strengths and weaknesses. If a strong signal for a NGB were obtained at hadron colliders one could proceed directly to measuring its couplings. However, if the only evidence for NGBs came from lepton colliders, where the evidence is indirect, determining the nature of the new physics is more complicated. To measure the couplings one would have to independently determine the NGB mass since coupling's values scale as $M_{Z'}^{-4}$. The recent review by Cvetic and Godfrey [9] summarizes the current status of NGB identification. For the most part existing studies of NGB identification have not included the limitations of using realistic detectors. This is especially important for hadron colliders. For lepton colliders virtually all existing studies examine how well couplings can be determined if the NGB mass is known. A main effort of the NGB subgroup was to extend existing studies to realistic detectors and to determining how well NGB properties could be determined in a model *blind* approach.

1. Hadron Colliders

Although the total Z' production cross section at a hadron collider is a function of the Z' couplings, the leptonic cross section depends on unknown contributions from supersymmetric particles or exotic fermions to the total width which makes its use as a tool to distinguish models questionable at best. The determination of Z' couplings is a daunting task due to large backgrounds and limited statistics. The most widely used observable for model identification at hadron colliders is the forward backward asymmetry, A_{FB}. Wulz examined this observable using rapidity bins. The results for the LHC are plotted for several models in Fig. 3. It is clear that these models would be distinguishable for $M_{Z'}$ up to about 3 TeV and depending on the ever, it is not clear as to what level one could extract precise coupling information.

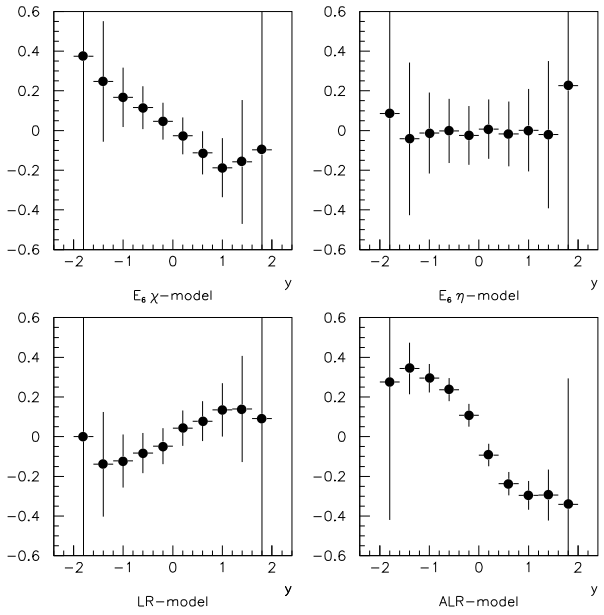

Figure 3: Z' asymmetries in dilepton channels at the LHC for $M_{Z'} = 2$ TeV. (From Ref. [16].)

2. Lepton Colliders

If either evidence for NGBs were observed at a hadron collider or deviations from the SM that could be interpreted as a NGB were observed at a Lepton collider, the measurement of the NGB couplings would be of primary importance. A number of contributions examined this problem for the NLC. Both Cuypers [18] and Riemann [19] assumed a specific Z' mass with the collider operating below this energy. In his analysis Cuypers [18] included polarization error, detector angular resolution, initial state radiation, and luminosity measurement errors. He assumed generic $v_{Z'}$ and $a_{Z'}$ couplings normalized to the charge of the electron e. For a $\sqrt{s} = 500$ GeV e^+e^- collider with $L = 50$ fb^{-1} operating in either e^-e^+ or e^-e^- mode, and assuming $M_{Z'} = 2$ TeV he found that $v_{Z'}$ and $a_{Z'}$ could be measured to about ± 0.3. Riemann [19] followed a similar approach but presented her results in terms of the couplings for specific NGB models and how well they could be discriminated. Riemann considered the NLC options; $\sqrt{s} = 500$ GeV $L = 50$ fb^{-1}, $\sqrt{s} = 1$ TeV $L = 100$ fb^{-1}, and $\sqrt{s} = 1.5$ TeV $L = 100$ fb^{-1}, with 80% electron polarization, detector angular acceptances, quark flavor tagging efficiencies, and luminosity measurement uncertainty of 0.05%. Riemann's results are summarized in Figure 4. It is clear from these results that the NLC will be able to extract leptonic coupling information for Z' masses up to $2-3\sqrt{s}$. It should be noted that the lepton observables only depend on products or squares of a'_f and v'_f which

Table I: New gauge boson search reaches in TeV. For the LRM $\kappa = 1$ is assumed, while for the UUM we take $s_\phi = 0.5$. Decays to SM fermions only are taken into account. The luminosities for the Tevatron, LHC, 60 TeV, and 200 TeV colliders are taken to be 10, 100, 100, 1000 fb^{-1}, respectively.

Machine	χ	ψ	η	SSM	LRM	ALRM	UUM	W'
Hadron Colliders								
CDF/D0	0.585	0.580	0.610	0.620	0.690	—	—	0.720
Tev33	1.0	1.0	1.0	1.1	1.1	1.2	1.1	1.2
LHC	4.6	4.1	4.2	4.9	4.5	5.2	4.6	5.9
60 TeV (pp)	13	12	12	14	14	15	14	20
60 TeV ($p\bar{p}$)	18	17	18	21	19	22	20	25
200 TeV (pp)	44	39	40	46	43	50	44	65
200 TeV ($p\bar{p}$)	64	62	65	69	65	75	65	83
Lepton Colliders								
NLC500	3.2	1.9	2.3	4.0	3.7	3.8	4.8	
NLC1000	5.5	3.2	4.0	6.8	6.3	6.7	8.2	
NLC1500	8.0	4.8	5.8	10	9.2	9.8	12	
NLC 5 TeV	23	14	17	30	26	28	35	
$\mu^+\mu^-$ 4 TeV	18	11	13	23	20	22	27	

results in a two-fold ambiguity in the signs of the couplings.

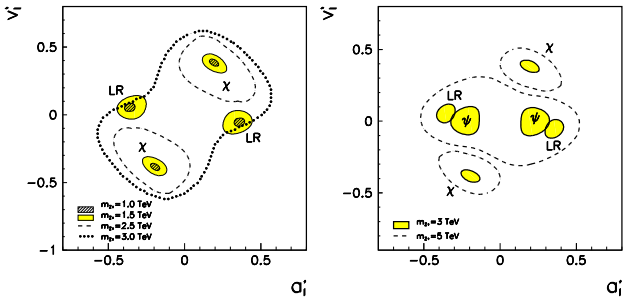

Figure 4: 95% C.L. contours for a'_ℓ and v'_ℓ. A Z' is assumed in the χ, ψ, or LR model for different Z' masses. The left and right figures are for $\sqrt{s} = 500$ GeV, $L = 50$ fb^{-1} and $\sqrt{s} = 1.5$ TeV, $L = 100$ fb^{-1}. (From Ref. [19].)

Riemann also studied model discrimination using heavy flavor tagging. The expected results for the $\sqrt{s} = 500$ GeV collider with $M_{Z'} = 1$ TeV are shown in Fig. 5. Riemann stresses that these results are sensitive to the systematic errors for the measurements on these final states.

Rizzo examined the capabilities of the NLC to determine both the mass as well as the couplings to leptons and b-quarks of Z''s below production threshold. This can be done by collecting data at several different values of $\sqrt{s}$. In his analysis he assumed e, μ, τ universality, 90% e^- polarization, 50% b-tagging efficiency, 0.25% luminosity measurement error, angular detector acceptance cut of $|\theta| > 10^o$, final state QED and QCD corrections are included, and neglecting t-channel exchange in $e^+e^- \to e^+e^-$. To insure model-independence the values of the Z' couplings $(v_{\ell,b}, a_{\ell,b})$ and $M_{Z'}$ were chosen randomly and anonymously. Performing the analysis for a wide range of possible mass and couplings then shows the power as well as the limitations of the technique. The results of one such analysis are shown if Fig. 6 where data was generated for $\sqrt{s} = 0.5$ 0.75, and 1 TeV with associated integrated luminosities of 70, 100, and 150 fb^{-1}. A 5-dimensional 95% C.L. allowed region for the mass and couplings is then found from a simultaneous fit of the various observables for the given energies. Figure 6 shows projections of the 5-dimensional region onto a 2-dimensional plane. To give these results a context, the expectations of several well-known Z' models are also shown. Rizzo's results again show the 2-fold ambiguity pointed out above. These results show that obtaining coupling information from different fermion species is important for discriminating between models. Rizzo also found that one needs at least 3 values of $\sqrt{s}$ to find $M_{Z'}$ and that spreading the integrated luminosities over too many Center of mass energies is also a failed strategy. A final note is that previous knowledge of the value of $M_{Z'}$ results in a much better measurement of the couplings.

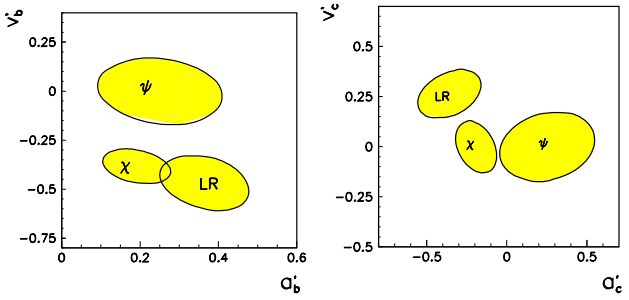

Figure 5: Model discrimination for $M_{Z'} = 1$ TeV at $\sqrt{s} = 0.5$ TeV with L=50 fb^{-1} for $e^+e^- \to b\bar{b}$ (left) and $e^+e^- \to c\bar{c}$ (right). 60% (40%) tagging efficiencies and 1% (1.5%) systematic errors were used for b (c). (From Ref. [19].)

Many theories beyond the SM of the electroweak and strong interactions predict the existence of new particles. For the purposes of this report, these new states can be organized into two major categories: exotic fermions and difermions. Other new particle possibilities consist of new gauge bosons and excited fermions; these are discussed elsewhere. For a broad overview and introduction to new particles, as well as original references, see [21] and the subgroup report by Berger and Merritt [22].

A. Overview

a) *Exotic Fermions.* New fermions are predicted by many gauge extensions of the SM and they often have the usual lepton and baryon number assignments while possessing non–canonical $SU(2)_L \times U(1)_Y$ quantum numbers, *e.g.*, the left–handed components are in weak isosinglets and/or the right–handed components in weak isodoublets. Fourth generation fermions are sometimes considered in this class although their quantum numbers are canonical. Some examples of these exotic fermions are as follows:

i) Vector fermions: These are present, for instance, in E_6 grand unified theories[23]. In this example, each fermion generation lies in the representation of dimension **27**, and in addition to the fifteen SM chiral fields, twelve new fields are needed to complete this representation. Among these, there will be two weak isodoublets of heavy leptons, one being right-handed and the other left-handed. Vector fermions can have SM invariant

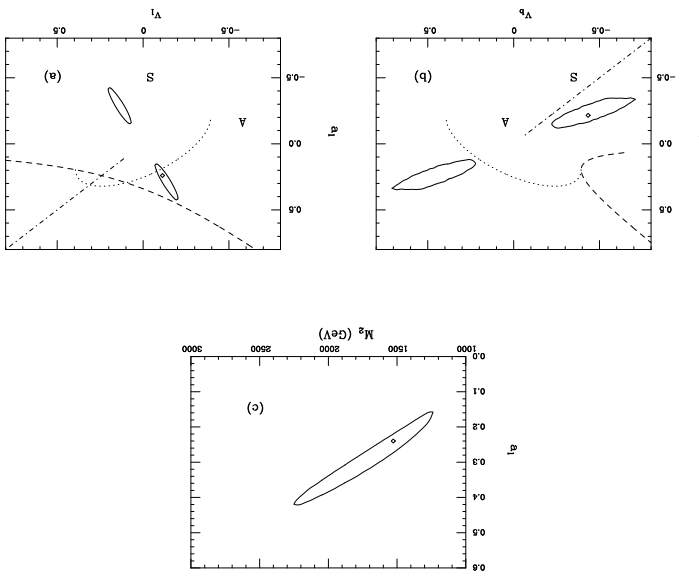

Figure 6: 95% CL allowed regions for the extracted values of the (a) lepton (b) b-quark couplings, and (c) $M_{Z'}$ for randomly selected Z' parameters compared to the predictions of the E_6 model (dotted), LR model (dashed), UUM (dash-dot), SSM (S), and ALR (A). For (c) only the $a_\ell > 0$ branch is shown. In all cases the diamond represents the corresponding input values.

ters which describe electroweak precision measurements[2].

ii) Mirror fermions: These have chiral properties which are opposite to those of ordinary fermions, i.e., the right-handed components are weak isodoublets and the left-handed ones are weak isosinglets. There is also a left-handed heavy neutrino. These fermions appear in many extensions of the SM and provide a possible way to restore left–right symmetry at the scale of electroweak symmetry breaking. They have many of the phenomenological difficulties associated with fourth generation fermions, such as the strict doublet mass splitting restrictions from contributions to the ρ parameter.

iii) Singlet fermions: These are the most discussed fermions in the literature, a prominent example being the right-handed neutrino in $SO(10)$. Indeed, in this unifying group, which is one of the simplest and most economic extensions of the SM, the smallest anomaly free fermion representation has dimension **16**. It contains the right-handed neutrino in addition to the 15 Weyl fermions in one fermion generation; with this neutrino being of the Majorana type. Singlet neutrinos, which can be either of Majorana or Dirac type, and new singlet quarks also occur in E_6 theories.

b) *Difermions.* These are scalar or vector particles which have unusual baryon and/or lepton number assignments. Examples of these particles are as follows:

i) Leptoquarks: These particles are color triplets with B= $\pm 1/3$ and L= ± 1. They naturally appear in models which place quarks and leptons on an equal footing, such as Technicolor, composite models (where quarks and leptons are made of the same subconstituents) as bound states of quark-lepton pairs, and also in GUTs (for example in E_6 or Pati-Salam SO(10) theories). We note that leptoquarks have recently returned to prominence in the literature due to the excess of high-Q^2 events in Deep Inelastic Scattering at HERA by both the ZEUS and H1[24] Collaborations. Leptoquarks have fixed gauge couplings to the photon, the W/Z bosons, and gluons (for spin–1 leptoquarks an anomalous chromo-magnetic moment may be present), and also *a priori* undetermined Yukawa couplings to lepton–quark pairs which determine their decays. For phenomenologically relevant leptoquarks, this Yukawa coupling should be chiral in order to, *e.g.*, restrain leptons from acquiring too large a magnetic moment and to prevent large violations in universality from π decay. In addition, they should essentially couple only to a single SM family to avoid problems with Flavor Changing Neutral Currents.

The interactions of leptoquarks can be described by an effective low-energy Lagrangian. The most general renormalizable $SU(3)_C \times SU(2)_L \times U(1)_Y$ invariant leptoquark-fermion interactions can be classified by their fermion number, $F = 3B + L$, and take the form[25]

$$\mathcal{L} = \mathcal{L}_{F=-2} + \mathcal{L}_{F=0}\,, \tag{1}$$

with

$$\begin{aligned}\mathcal{L}_{F=-2} \;=\; & (g_{1L}\bar{q}_L^c i\tau_2 \ell_L + g_{1R}\bar{u}_R^c e_R) S_1 + \tilde{g}_{1R}\bar{d}_R^c e_R \tilde{S}_1 \\ & + g_{3L}\bar{q}_L^c i\tau_2 \vec{\tau} \ell_L \vec{S}_3\end{aligned}$$

$$+\tilde{g}_{2L}\bar{u}^c_R\gamma^\mu\ell_L\tilde{V}_{2\mu} + h.c.\,, \qquad (2)$$

$$\mathcal{L}_{F=0} = (h_{2L}\bar{u}_R\ell_L + h_{2R}\bar{q}_L i\tau_2 e_R)R_2 + \tilde{h}_{2L}\bar{d}_R\ell_L\tilde{R}_2$$
$$+(h_{1L}\bar{q}_L\gamma^\mu\ell_L + h_{1R}\bar{d}_R\gamma^\mu e_R)U_{1\mu}$$
$$+\tilde{h}_{1R}\bar{u}_R\gamma^\mu e_R\tilde{U}_{1\mu} + h_{3L}\bar{q}_L\vec{\tau}\gamma^\mu\ell_L\vec{U}_{3\mu} + h.c.$$

Here, q_L and ℓ_L denote the $SU(2)_L$ quark and lepton doublets, respectively, while $u_R\,, d_R$ and e_R are the corresponding singlets. The indices of the leptoquark fields indicate the dimension of their $SU(2)_L$ representation. The subscripts of the coupling constants label the lepton's chirality. For an overview of the phenomenology associated with a light, HERA-inspired leptoquark see for example [8] and references therein.

ii) Diquarks: These particles have B= $\pm 2/3$ and L= 0, and are also predicted in composite models as bound states of quark pairs, and in Grand Unified models (*e.g.*, the model based on the E_6 symmetry group).

iii) Bileptons: These particles have B= 0 and L= $0, \pm 2$. They occur in, *e.g.*, theories where the electroweak gauge group for leptons is extended from $SU(2)_L \times U(1)_Y$ to $SU(3)$ and baryon and lepton numbers are conserved. They may carry either 0 or 2 units of lepton number and no baryon number. Bileptons can appear both as scalar and as vector gauge particles and can be singly or doubly charged; for instance, doubly charged dilepton gauge bosons appear in $SU(15)$ GUTs. Bileptons have couplings to ordinary gauge bosons which are fixed by gauge invariance, and Yukawa couplings to leptons which mediate their decays. For a detailed survey, see Cuypers and Davidson[26].

Clearly the possible set of new particles is so large that we cannot hope to examine production signatures and search reaches for all of the above at future hadron and lepton colliders and so we will concentrate on the new work that was performed at Snowmass on just a few of these possibilities: leptoquark production at lepton and hadron colliders, bilepton production at the NLC, and neutral heavy lepton production at lepton colliders. For a summary of older work on this subject, see Ref. [21].

B. New Particle Production at Colliders

At hadron colliders the best way to search for leptoquarks is through the pair production process $q\bar{q}, gg \to LQ\overline{LQ}$ with the on-shell leptoquarks then decaying into (1) two jets plus charged leptons, (2) two jets, one charged lepton and missing energy or (3) two jets plus missing energy. Clearly the SM backgrounds increase as we go from (1) to (3) making discovery difficult. In most analyses, leptoquarks are considered to be produced 'one at a time', *i.e.*, the fact that they may lie in nearly degenerate multiplets is usually ignored. Fortunately, all leptoquark multiplets lead to a rather high branching fraction, $B \geq 0.5$, into the charged lepton mode as can be observed by an examination of the Lagrangian above. For scalar, *i.e.*, spin-0 leptoquarks the cross section depends solely on their mass in the limit that the $q\ell LQ$ Yukawa coupling, λ, is of electroweak strength or less, *i.e.*, $\tilde{\lambda} = \lambda/e < 1$. In the vector(spin-1) case the situation is somewhat less clear. If vector leptoquarks are gauge particles then the cross section depends solely on their mass. However, it possible that the cross section may depend on one or more additional parameters such at the anomalous chromomagnetic moment, κ. Note that for the case where vector leptoquarks are gauge particles κ is fixed to unity.

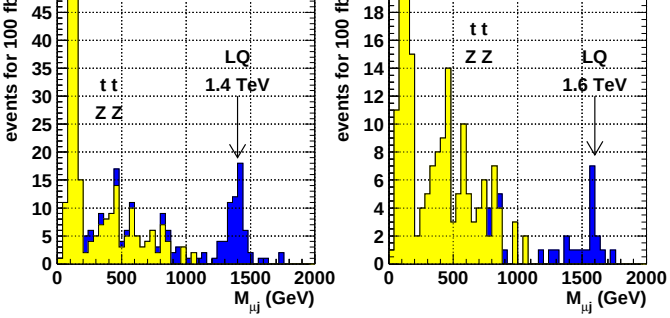

Figure 7: Leptoquark signal and background mass distribution for second generation leptoquarks for the CMS detector. (From Ref. [28].)

The production of both scalar and vector leptoquarks at the Tevatron and LHC have been previously discussed in the literature. Rizzo updated[27] these analyses and extended them to TeV33 and possible higher energy hadron colliders at $\sqrt{s} = 60, 200$ TeV. As is well-known, hadron colliders can distinguish scalar from vector leptoquarks from the size of the cross section, and perhaps tell us something about their charged lepton branching fraction as well. However, we cannot learn about the leptoquark's electroweak interactions at a hadron collider. For leptonic branching fractions of unity and a conservative assumption about the number of required signal events the search reaches for scalar leptoquarks were found to be 0.35(1.34, 4.9, 15.4)TeV at TeV33, LHC and the two higher energy colliders, respectively, assuming that they ran in pp mode. The corresponding reaches for gauge boson vector leptoquarks was found to be 0.58(2.1, 7.6, 24.2)TeV. At the LHC a detailed study of second generation scalar leptoquark pair production was performed using the CMS detector fast Monte Carlo[28] in order to understand backgrounds and finite resolution effects. The results are shown in Fig. 7, where we see that the search reach may be as high as $M_{LQ} = 1.6$ TeV.

Another possibility which is not often discussed is the single production of leptoquarks vis gq fusion, *i.e.*, $gq \to LQ + \ell$ where ℓ is either a charged lepton or a neutrino. The cross section for this depends quadratically on the unknown Yukawa coupling $\tilde{\lambda}$. For sizeable values of $\tilde{\lambda}$ this process will dominate pair production. For very small values of $\tilde{\lambda}$ it is clear that the pair production cross section is far larger even though a pair of heavy objects is being produced. However, the single production process allows one to study the size of the Yukawa coupling for a leptoquark which has already been observed through the pair production mechanism. For example, Fig. 8 shows the single production cross section for a scalar leptoquark at a $\sqrt{s} = 100$ TeV collider for very small values of $\tilde{\lambda}$. For luminosities in the $100 - 1000 fb^{-1}$ range very large event rates are obtained for

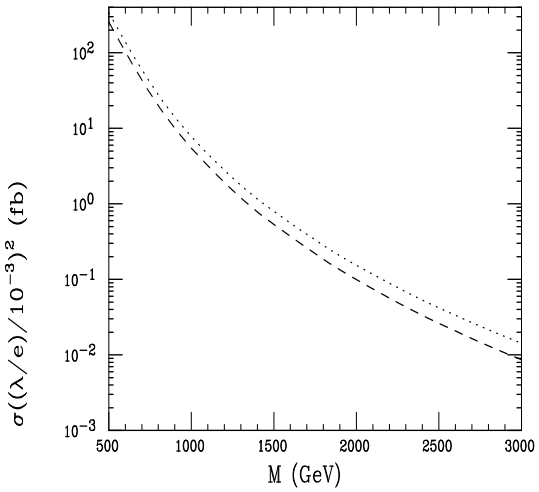

Figure 8: Single scalar leptoquark production cross sections at a 100 TeV pp collider as functions of the leptoquark mass, for both the gu (dotted) and gd (dashed) intial states. The overall Yukawa coupling has been rescaled to units of $\tilde{\lambda}/10^{-3}$.

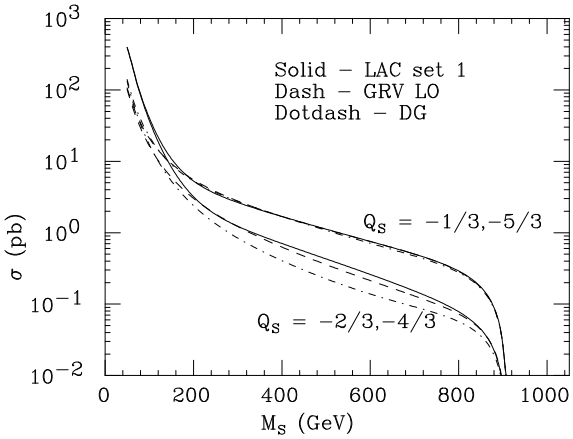

Figure 9: The cross sections for leptoquark production due to resolved photon contributions in $e\gamma$ collisions. The photon beam is due to laser backscattering in a $\sqrt{s} = 1000$ GeV collider. The different curves correspond to different photon distribution functions (from Ref. [29].)

Leptoquarks can also be pair produced at lepton colliders. As is well known, their production characteristics yield complete information about their spin and all of their electroweak quantum numbers. The only difficulty is that the pair production reach is limited by $\sqrt{s}/2$ and thus much attention has focussed on single production of leptoquarks via γe collisions through either the Weisacker-Williams process or at a true photon-electron collider employing the backscattered laser technique. As shown in Fig. 9 from Doncheski and Godfrey[29], for electromagnetic strength Yukawa couplings the search reach is significantly extended in either case and that polarization asymmetries can be used to determine the leptoquarks quantum numbers. Of course this approach fails if the Yukawa couplings are substantially smaller that this assumed strength.

If very heavy leptoquarks exist then they may be searched for indirectly in $\ell^+\ell^- \to q\bar{q}$ since they constitute new $t-$ or $u-$channel exchanges. Again the potential size of their influence is controlled by the size of their Yukawa couplings. By combining angular and polarization asymmetries as well as the total cross section it is possible to examine which regions of the Yukawa coupling-LQ mass plane would show such sensitivity. This case was analyzed in detail by Berger[30] for the generic scalar leptoquark scenario. Assuming either right- or left-handed couplings for the scalar leptoquark and electromagnetic coupling strength for the Yukawa couplings, both the NLC and the NMC were found to be able to probe scalar leptoquark masses in the range $1.5-2\sqrt{s}$ assuming canonical luminosities.

Cuypers and Davidson[26] have performed a comprehensive examination of the search reach for bileptons at the NLC in the $\gamma\gamma$, γe, e^+e^- and e^-e^- collider modes. All of these modes provide a reach up to the kinematic limit and can yield detailed information on the bilepton quantum numbers and Yukawa coupling structure. Using various modes, the reach for bileptons at the NLC with canonical luminosities was found to be $m_{BL} \geq 50\lambda_{ee}\sqrt{s}$ where λ_{ee} is the bilepton coupling to ee, as displayed in Fig. 10.

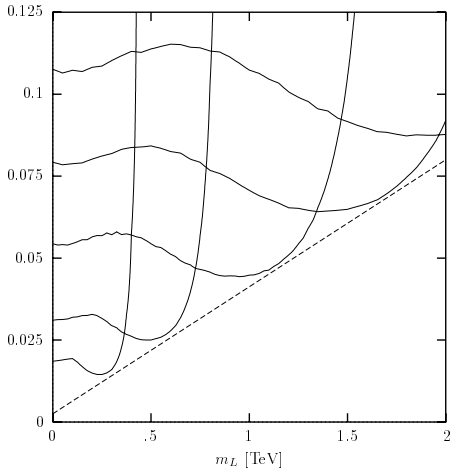

Figure 10: Smallest observable scalar bilepton coupling as a function of the bilepton mass at the level one standard deviation in $e\gamma$ processes. The assumed e^+e^- center of mass energies are 0.5, 1, 2, and 3 Tev, from left to right. (From Ref. [26].)

Kalyniak and Melo[31] studied the single production of neutral heavy leptons in association with a massless neutrino at lepton colliders. These particles may be produced either by $s-$channel Z exchange and/or by W exchange in the $t-$channel depending on the leptonic flavor. These authors concentrated on a model where every generation has a massless neutrino as well

in terms of the heavy lepton masses and a set of mixing parameters which describe the experimentally allowed size of the violation of unitarity due to mixing amongst all 6 neutrinos in the 3×3 light neutrino basis. For mixing parameters as large as allowed by current experiment the search reaches were found to extend out to the kinematic limit of a given machine as shown in Fig. 11. For masses well inside the kinematic limit, extremely small values of the mixing parameters, of order $10^{-(4-6)}$, were found to be accessible.

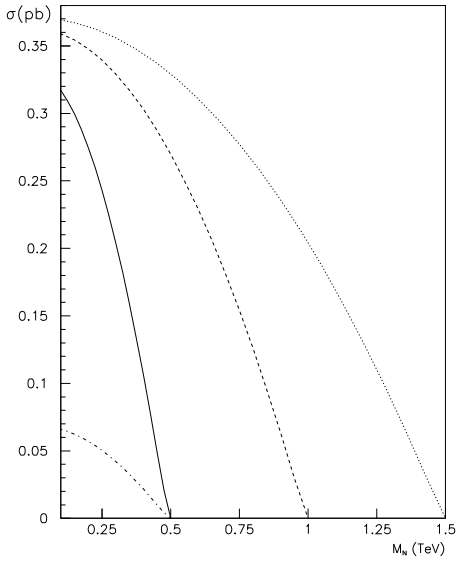

Figure 11: Total cross section vs the neutral heavy lepton mass M_N for e^+e^- collider at three different energies: $\sqrt{s} = 0.5$ TeV (solid line), $\sqrt{s} = 1.0$ TeV (dashed line), and $\sqrt{s} = 1.5$ TeV (dotted line) and for $\mu^+\mu^-$ collider at $\sqrt{s} = 0.5$ TeV (dash-dotted line); $ee_{mix} = 0.0071$, $\mu\mu_{mix} = 0.0014$, $\tau\tau_{mix} = 0.033$ (from Ref. [31]).

Heavy neutrinos of the Majorana type are perhaps best probed in e^-e^- collisions since the initial state has $L = 2$. It was pointed out many years ago[32] that heavy Majorana neutrinos, exchanged in the $t-$ and $u-$channels, might mediate the process $e^-e^- \to W^-_{L,R}W^-_{L,R}$ at an observable rate. Since that time there has been some controversy concerning whether large rates can be obtained in the case where the SM gauge group is not augmented due to constraints from other processes, such as the lack of the observation of neutrinoless double beta decay. There were two overlapping analyses presented at Snowmass on this subject by Heusch[33] and by Greub and Minkowski[34], who both advocate models where large rates may be obtainable for suitable ranges of the parameters. In particular, Heusch points out the rather large theoretical uncertainties in the nuclear physics aspects of double beta decay in the limit that highly massive objects are being exchanged, *i.e.*, in the truly short-distance limit. Heusch argues that a number of quark-level inhibition factors arise in this case, which when combined reduce the size of the neutrinoless double beta decay matrix element by more than a factor of 40. This substantially enlarges the parameter space for which large rates may be obtained. Greub and Minkowski show in a very detailed analysis that the size of the resulting cross section can be large and they demonstrate that the backgrounds from the more conventional SM processes are small and can be controlled by both beam polarization and various kinematic cuts.

As a summary of new particle production we display in Table II the search reaches obtainable at various colliders for the particles surveyed here. We note that where the listed discovery limit is larger than $\sqrt{s}$, we have included the reach from indirect effects. The question marks in the Table indicate that a detailed study has not yet been performed. Figure 12 presents the search reach for new particles decaying into dijets at the Tevatron, for several possible scenarios[35]. We see here that large integrated luminosities will reach the TeV range.

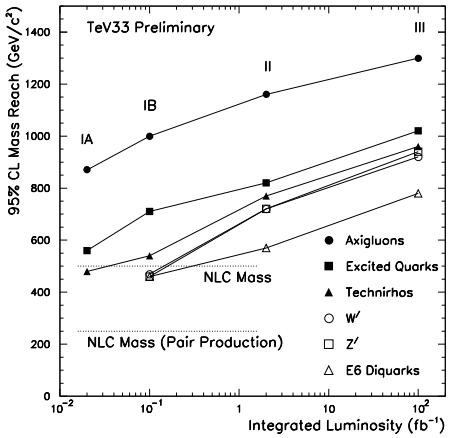

Figure 12: The 95% C.L. mass reach for new particles decaying into dijets as a function of luminosity at the Tevatron.

IV. NEW INTERACTIONS

Without knowing what physics lies beyond the standard model we can take several distinct approaches. In previous sections we explored the phenomenology of specific manifestations of new physics. In this section we take a more generic approach; looking for new physics via the effect they have on interactions well below their typical scales. First we consider models of dynamical symmetry breaking and their "low energy" particle spectrum. Quite generally, if a low mass Higgs boson does not exist and the weak sector becomes strongly interacting at high energy a whole spectrum of states should exist, similar to the low lying particle spectrum of QCD. This subject was studied in detail by another Snowmass working group [36]. However, several members of the new phenomena working group also examined the phenomenology of specific examples of this scenario; one-family technicolor and topcolor assisted technicolor. Secondly, we take this progression to its conclusion, that new particles are not observed and new physics only manifests itself through the existence of effective interactions at low energy. For the detailed report see the subgroup summary by Cheung and Harris[37].

Table II: New particle discovery reaches in TeV at future colliders. The luminosities for TeV33(LHC, 500 GeV NLC, 1 TeV NLC) are assumed to be 10(100, 50, 100)fb^{-1}, respectively. In the case of LQ's at the NLC, the first(second) value is for pair production (single production with electromagnetic strength Yukawa couplings). The third value is the indirect reach in the later case. The question mark indicates that a Monte Carlo study has not yet been performed.

Particle	TeV33	LHC	500 GeV NLC	1 TeV NLC
Scalar LQ	0.33	1.6	0.25,0.45,5.0	0.5,0.9,6.5
Vector LQ	~ 0.5	~ 2.2	0.25,0.45,3.0	0.5,0.9,5.5
Axigluon	1.3	~ 5.0	0.4	0.8
Heavy Q	?	?	0.25	0.5
Heavy L	?	?	0.25	0.5
Diquark	$0.2 - 0.78$	~ 5	0.25	0.5
Bilepton	-	-	0.45	0.9

A. One-Family Technicolor

Eichten and Lane [38] described a one-family technicolor model with color triplet techniquarks and color singlet technileptons. The techniquarks bind to form color singlet technirhos, $\rho^{\pm}_{T1}$ and ρ^{0}_{T1}, with mass roughly in the range 200 to 400 GeV. Color singlet technirhos can be produced in hadron collisions through quark-antiquark annihilation. The expected decay modes are $\rho^{\pm}_{T1} \rightarrow W^{\pm}Z$, $W^{\pm}\pi^{0}_{T}$, $Z\pi^{\pm}_{T}$, $\pi^{\pm}_{T}\pi^{0}_{T}$ and $\rho^{0}_{T1} \rightarrow W^{\pm}W^{\mp}$, $W^{\pm}\pi^{\mp}_{T}$, $\pi^{\pm}_{T}\pi^{\mp}_{T}$. The technipions, π_T, in turn decay predominantly to heavy flavors: $\pi^{0}_{T} \rightarrow b\bar{b}$, and $\pi^{\pm}_{T} \rightarrow c\bar{b},\ t\bar{b}$. Techniquarks will also bind to form color octet technirhos, ρ^{0}_{T8} with mass roughly in the range 200 to 600 GeV. Color octet technirhos are produced and decay via strong interactions. If the mass of the colored technipions is greater than half the mass of the technirho, then the ρ^{0}_{T8} will decay predominantly to dijets: $\rho_{T8} \rightarrow gg$. If colored technipions are light the ρ^{0}_{T8} decays to pairs of either color triplet technipions (leptoquarks) or color octet technipions.

1. $\rho_{T1} \rightarrow W + dijets$ at the Tevatron

The search for $\rho_{T1} \rightarrow WX$, where $X = W,\ Z$, or π_T, is sufficiently similar to the search for a massive W' decaying to WZ that Toback [39] was able to extrapolate the W' search to higher luminosities as an estimate of the search limits for color singlet technirhos at the Tevatron. He considered the decay chain $\rho_T \rightarrow WX \rightarrow e\nu + dijets$, and required both the electron and neutrino to have more than 30 GeV of transverse energy, E_T. He required at least two jets in the event, one with $E_T > 50$ GeV and the other with $E_T > 20$ GeV. The resulting $W + dijet$ mass distribution from 100 pb^{-1} of CDF data was in good agreement with standard model predictions and was used to determine the 95% C.L. upper limit on the ρ_{T1} cross section, shown in Fig. 13. The acceptance for the technirho was assumed to be roughly the same as for a W'. The extrapolation to higher luminosities shows that TeV33 (30 fb^{-1}) should be able to exclude a color singlet technirho decaying to $W + dijets$ up to roughly 400 GeV at 95% C.L.. This covers the expected range in the one family technicolor model.

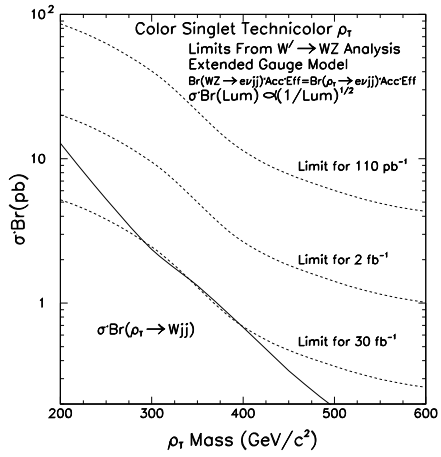

Figure 13: 95% CL upper limit of $\sigma \cdot Br(\rho_T \rightarrow Wjj)$ vs M_{ρ_T}. The solid line is the theoretically expected $\sigma \cdot Br$ and assumes $\rho_{T1} \rightarrow WX \rightarrow Wjj = 100\%$. The dashed lines show predicted limits for 100 pb^{-1}, 2 fb^{-1}, and 30 fb^{-1} respectively. (From Ref. [39].)

2. $\rho_{T1} \rightarrow W + b\bar{b}$ at the Tevatron and LHC

Womersley [40] studied the process $q\bar{q}' \rightarrow \rho_{T1} \rightarrow W\pi_T \rightarrow (l\nu)(b\bar{b})$, including the effect of tagging events with a final state b quark, for the particular case of $M_{\rho_T} = 210$ GeV and $M_{\pi_T} = 115$ GeV. The signal is a W (reconstructed from $l+ \not{E}_T$) and two jets with a resonance in the dijet mass m_{jj}. The backgrounds are $W + jets$ and $t\bar{t}$. Womersley generated signal and background events using ISAJET and used a fast simulation of the CMS detector at the LHC. Events are required to have a good W candidate in $l\nu$ mode and two jets with $E_T > 20$ GeV and $|\eta| < 2.5$. The single b-tagging efficiency was assumed to be 50% with a mistag rate of 1% for light quark jets. Fig. 14 shows the reconstructed π_T peak in the signal sample, and that prior to b-tagging the signal is swamped by the large QCD $W + jj$ background. Fig. 14 also shows that after b-tagging the signal to background is significantly improved at both the

Tevatron but the rate at the LHC is considerably higher. Clearly, b-tagging is important to reduce the $W + jets$ background.

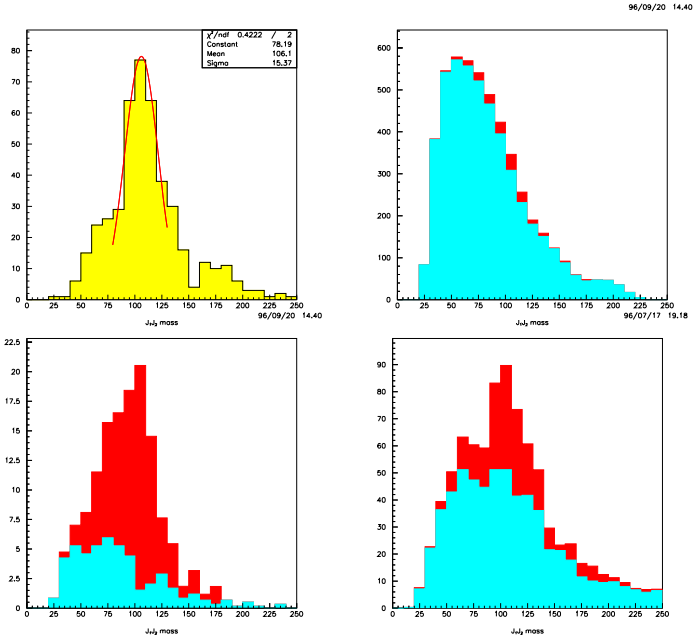

Figure 14: $\rho_{T1} \to W + \pi_T \to (l\nu)(b\bar{b})$ search. (upper left) Leading dijet invariant mass distribution for signal at the LHC. (upper right) Same for signal (dark) and background (light) at the Tevatron before b-tagging. Vertical scale is events/10 GeV/2 fb^{-1}. (lower left) Same at the Tevatron after b-tagging. (lower right) Same at the LHC after b-tagging. Vertical scale is events/10 GeV/0.5 fb^{-1}. All horizontal scales are in GeV. (From Ref. [40].)

3. $gg \to Z_L Z_L,\ W_L W_L$ at the LHC

Lee [41] studied the production of longitudinal gauge boson pairs via gluon fusion in the one-family technicolor at the LHC. Fig. 15 shows that when the invariant mass is above the threshold for production of pairs of colored technipions, the $W_L W_L$ or $Z_L Z_L$ signal cross section is greater than the standard model background by over an order of magnitude. Assuming an integrated luminosity of 100 fb^{-1}, the $Z_L Z_L$ signal, with over a thousand events in the four lepton final state (e and μ), will be easily observable.

B. Topcolor Assisted Technicolor

Theories of dynamical electroweak symmetry breaking, such as extended technicolor (ETC), have difficulty in generating large fermion masses, particularly m_t. This is circumvented in top quark condensation models, where the massive top quark is acquired from $\langle \bar{t}_L t_R \rangle$; however these dynamics alone do not fully break the electroweak symmetry. The necessary ingredients to accomplish both tasks are present in Topcolor assisted technicolor[42], where electroweak interactions are broken via technicolor with ETC, and the large top quark mass is obtained

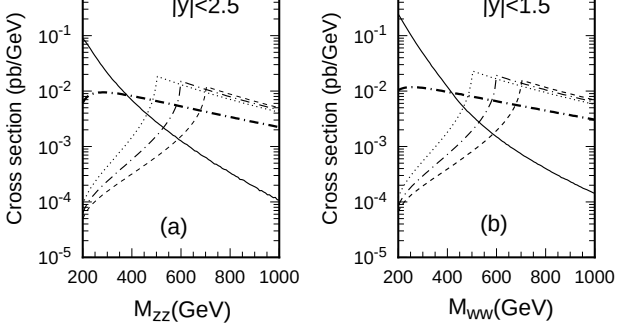

Figure 15: The cross sections for (a) Z_L-pair and (b) W_L pair production via gluon fusion in pp collisions at $\sqrt{s} = 14$ TeV. The solid curves are for the $q\bar{q}$ initiated backgrounds, and dotted, dot-dashed, and dashed curves are for technipion masses of 250 GeV, 300 GeV, and 350 GeV respectively. The thick dot-dashed curves are for the chiral limit ($m_{\pi_T} = 0$). (From Ref. [41].)

from the combination of ETC and a dynamical condensate. In this case the new strong dynamics is a result of an extended gauge sector which generates the four fermion interaction

$$\frac{g^2}{\Lambda^2} \bar{\psi}_L t_R \bar{t}_R \psi_L \,, \tag{3}$$

where ψ_L is the third generation $SU(2)_L$ quark doublet and $\Lambda \simeq \mathcal{O}(1\,\mathrm{TeV})$ is the typical scale of the new interactions. The SM gauge group is thus enlarged to

$$SU(3)_1 \times SU(3)_2 \times U(1)_1 \times U(1)_2 \to SU(3)_C \times U(1)_Y \,, \tag{4}$$

where the $SU(3)_1$ and $U(1)_1$ couple strongly to the third generation. The breaking of the $SU(3)$ factors gives rise to a set of massive degenerate color octet bosons, B^a_μ, with masses $\lesssim 2\,\mathrm{TeV}$, as well as the usual massless gluons. Here we denote the massive color octet as topgluons, but they are sometimes referred to as colorons in the literature[43]. Additional interactions, represented in this model by the extra $U(1)$ factor, must also be present in order to avoid b-quark condensation. (This can also be achieved in axial Topcolor models, where the b_R field does not couple to the $SU(3)_1$, however this possibility will not be discussed here.) The additional $U(1)$ gives rise to a Topcolor Z' boson, which is expected to have mass $\lesssim 2 - 3\,\mathrm{TeV}$. Constraints on this Z' from electroweak precision measurements have been considered in Ref. [44], with the result that $M_{Z'} \gtrsim 0.5 - 1.5\,\mathrm{TeV}$ for small values of the $U(1)$ mixing angle.

Harris[45] has examined the production of topgluons, decaying into $t\bar{t}$, as well as the QCD background for this process, and has included the projected experimental efficiency for reconstructing the $t\bar{t}$ final state, in order to estimate the topgluon search reach in a $t\bar{t}$ resonanant state. The results are presented in Fig. 16, assuming that the width of the topgluon is given by $0.3M$, where M represents the mass of the topgluon. We see that the discovery reach probes the Tev scale for luminosities > 2 fb^{-1}.

color Z' bosons at the Tevatron, by examining the decay chain $Z' \to t\bar{t} \to \ell\nu b\bar{b}jj$. Using PYTHIA Monte Carlo, CDF detector simulation, and full reconstruction for both signal and background, she obtains the results displayed in Fig. 17a. Here, a potential 5σ resonance signal is compared to the expected Z' production cross section. We see that the search reach for a narrow Z' approaches the TeV scale at TeV33. Rizzo examined[10] the indirect search reach for a topcolor Z' at the NLC. The results are shown in Fig. 17b, where we see that topcolor Z' bosons with masses in excess of 4.5 TeV may be discerned from examining charm and top quark pair final state production. This explores the entire expected mass region for the existence of these particles.

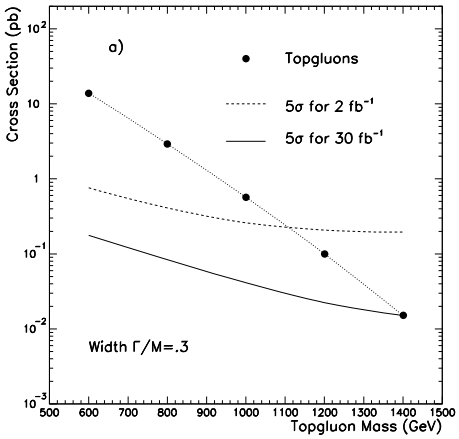

Figure 16: The mass reach for $t\bar{t}$ decays of topgluons of width 0.3 M. The production cross section (points) is compared to the 5σ reach at the Tevatron with 2 fb^{-1} (dashed) and 30 fb^{-1} (solid).

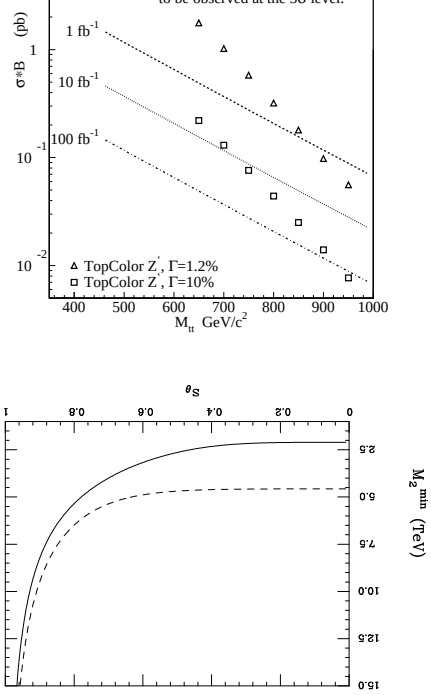

Figure 17: Topcolor Z' search reach at (a) TeV33 as a function of its mass, where the width is assumed to be 0.012M (triangles) or 0.1M (squares). (b) a 500 GeV NLC with 50 fb^{-1}, where the solid lines include data from e, μ, τ and b final states, and the dashed curve also includes data on c and t.

C. Effective Operators

As we have seen in previous sections, new physics can show up either through the direct production of new particles or through deviations of precision measurements from their standard model predictions. A powerful and systematic approach to parametrizing the effects of new physics is to use an effective Lagrangian ($\mathcal{L}_{eff}$) with the various terms ordered in terms of an energy expansion of the scale of new physics:

$$\mathcal{L}_{eff} = \mathcal{L}_0 + \frac{1}{\Lambda}\mathcal{L}_1 + \frac{1}{\Lambda^2}\mathcal{L}_2 + \ldots \qquad (5)$$

In this approach, an effective Lagrangian obeys the SM symmetries and is constructed out of the SM fields. The leading terms are given by the SM while the coefficients of higher dimension operators parametrize the effects of new physics. The effective Lagrangian for an analysis of new interactions was written down by Buchmüller and Wyler [46]. Specific examples of new physics will modify the coefficients of $\mathcal{L}_{eff}$ in unique patterns characteristic of the new physics. For example, Layssac *et al.* have shown that the existence of a Z' would result in a unique pattern of deviations [47]. Thus, if deviations were observed the pattern would give important clues to the underlying physics. In this section we follow this approach to find how precisely future colliders can measure several of the terms in $\mathcal{L}_{eff}$. While we concentrate on specific terms, related analysis putting constraints on other types of new physics can be found in reports of the Strongly Interacting Weak Sector working group.

1. Contact Interactions

Contact, or four Fermi, interactions have long been used to parametrize the effects of fermion substructure as form factors or the residual effects of constituent binding forces. Nevertheless one of the first manifestations of contact interactions was Fermi decay with its characteristic coupling, G_F, having dimensions of inverse mass squared and which we now know to be a low energy approximation to W-boson exchange. In a previous section we saw how the effects of new gauge bosons could be observed through deviations of precision measurements with contact terms proportional to $1/M_{Z'}^2$ (for a fixed $\sqrt{s}$). One can imagine that contact interactions can signal many other types of new physics. So we see that contact interactions can indicate many types of physics beyond the standard model, with the pattern of new interactions pointing to the nature of the new physics.

In this subsection we consider contact interactions for

of dimension 6, can be written most generally as

$$\mathcal{L} = \frac{g_{eff}^2 \eta}{2\Lambda^2}\left(\bar{q}\gamma^\mu q + \mathcal{F}_\ell \bar{\ell}\gamma^\mu \ell\right)_{L/R}\left(\bar{q}\gamma_\mu q + \mathcal{F}_\ell \bar{\ell}\gamma_\mu \ell\right)_{L/R}, \quad (6)$$

where the generation and color indices have been suppressed, $\eta = \pm 1$, and $\mathcal{F}_\ell$ is inserted to allow for different quark and lepton couplings but is anticipated to be $\mathcal{O}(1)$. Since when these operators are used to parametrize substructure, the binding force is expected to be strong when Q^2 approaches Λ, it is conventional to define $g_{eff}^2 = 4\pi$. However, it should be remembered that if other types of new physics give rise to these operators, g^2 could be much smaller. The subscript L/R indicates that the currents in each parenthesis can be either left- or right-handed and various possible choices of the chiralities lead to different predictions for the angular distributions of the reactions where the contact terms contribute. Contact interactions can affect jet production, the Drell-Yan process, lepton scattering etc. Compared to the SM, the contact interaction amplitudes are of order $\hat{s}/\alpha_s\Lambda^2$ or $\hat{s}/\alpha_{em}\Lambda^2$ so the effects of the contact interactions will be most important at large $\hat{s}$.

$\ell\ell\ell'\ell'$ Contact Terms: Cheung, Godfrey, and Hewett [48] studied $\ell\ell\ell'\ell'$ contact interactions at future e^+e^- and $\mu^+\mu^-$ colliders and derived limits on the new physics scale Λ using the reactions $e^+e^- \to \mu^+\mu^-$ and $\mu^+\mu^- \to e^+e^-$. For illustration, we show in Fig. 18, the $\cos\theta$ distribution for $e^+e^- \to b\bar{b}$ at $\sqrt{s} = 0.5$ TeV for the SM and with the contact term present for $\eta = 1$ and various values of Λ. The effects of the contact term are qualitatively similar for other final states. To obtain the sensitivity to the compositeness scale they set $\eta = \pm 1$ and performed a χ^2 analysis, comparing the angular distributions for a finite value of Λ to the SM predictions. The detector acceptance was taken to be $|cos\theta| < 0.985$ for the e^+e^- collider and $|cos\theta| < 0.94$ for the $\mu^+\mu^-$ collider. The angular distribution was divided into 10 equal bins. The 95% CL that can be obtained on Λ are given in Table III. The sensitivity to Λ in contact interactions was found to range from 10 to 50 times the center of mass energy. Polarization in the e^+e^- colliders gives slightly higher limits than those obtained at unpolarized $\mu^+\mu^-$ colliders of the same energy.

In addition to the e^+e^- mode, Kumar examined the physics reach of fixed target Moller scattering at the NLC [49]. He found that Λ_{ee} could be probed to roughly 50 TeV in this manner.

$\ell\ell q\bar{q}$ Contact Terms: Cheung, Godfrey, and Hewett [48] also considered the $\ell\ell q\bar{q}$ contact interactions at future e^+e^- and $\mu^+\mu^-$ colliders. They restricted themselves to $\ell\ell c\bar{c}$ and $\ell\ell b\bar{b}$ terms where the heavy flavor final states can be tagged. They used the same χ^2 analysis described above and assumed flavor tagging efficiencies of $\epsilon_b = 60\%$ and $\epsilon_c = 35\%$ ($\epsilon_b = 60\%$ and $\epsilon_c = 35\%$) for the e^+e^- ($\mu^+\mu^-$) colliders. They found that using polarized e^- beams could probe slightly higher mass scales than the $\mu^+\mu^-$ case, and were potentially very important for disentangling the chiral structure of contact terms if they cies at e^+e^- colliders results in higher limits for $\Lambda(\ell\ell q\bar{q})$ than can be obtained at $\mu^+\mu^-$ colliders (up to a factor of two for the $c\bar{c}$ case). These results are included in Table III.

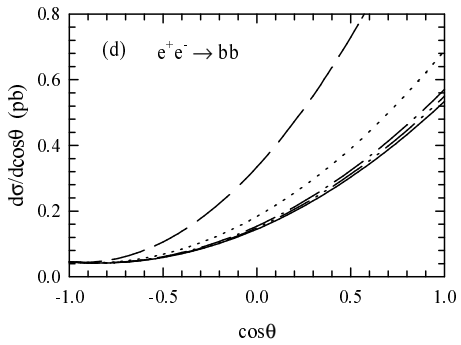

Figure 18: The $\cos\theta$ distribution for unpolarized $e^+e^- \to b\bar{b}$ at $E_{CM} = 0.5$ TeV. The solid line is for the SM ($\Lambda = \infty$). Unpolarized e^+e^- with $\eta_{LL} = +1$. Dashed line for $\Lambda = 5$ TeV, dotted line for $\Lambda = 10$ TeV, dot-dashed for $\Lambda = 20$ TeV, and dot-dot-dashed for $\Lambda = 30$ TeV.

P. de Barbaro *et al* [50] studied the effect of a left handed contact interaction between quarks and leptons at the Tevatron. They compared the invariant mass distribution of $\ell\bar{\ell}$ pairs produced in Drell-Yan production for the SM with that obtained assuming a left-handed $q\bar{q}\ell\bar{\ell}$contact interaction for various values of the scale, Λ. A contact interaction would result in an enhancement of the dilepton differential cross section at high invariant mass. Fig. 19 shows the Drell-Yan cross section for various values of the scale $\Lambda_{LL}^-(ee)$. Barbaro *et al* estimated the sensitivity of Tevatron measurements with higher luminosities using Monte Carlo simulations. Using 110 pb^{-1} of CDF data on dielectron production they report preliminary limits of $\Lambda_{LL}^-(q\bar{q} \to e^+e^-) \geq 3.4$ TeV and $\Lambda_{LL}^+(q\bar{q} \to e^+e^-) \geq 2.4$ TeV at 95% CL. Combined with the dimuon channel they obtain limits about 0.5 TeV more stringent than with electrons alone. Assuming present detector performance, with 30 fb^{-1} of integrated luminosity for TeV33 the Tevatron will be sensitive to $\Lambda_{LL}^+ \leq 14$ TeV and $\Lambda_{LL}^- \leq 20$ in the ee channel.

$q\bar{q} \to q\bar{q}$ Contact Terms: An excess of events with high E_T jets in hadron collisions is a well known signature for $q\bar{q} \to q\bar{q}$ contact interactions. However the uncertainties in the parton distributions, ambiguities in QCD calculations, and uncertainties in jet energy measurement make it difficult to discover a $qq \to qq$ contact interaction. Another signal of $qq \to qq$ contact interactions which is not very sensitive to these problems is a dijet angular distribution which is more isotropic than predicted by QCD. Using this approach gives the limits on new physics scales given in Table II [51, 52].

$q\bar{q} \to \gamma\gamma$ Contact Terms: The lowest dimension gauge invariant operator involving two fermions and two photons is a dimension 8 operator which induces a $q\bar{q}\gamma\gamma$ contact interaction. Assuming parity and CP conservation, this interaction is given

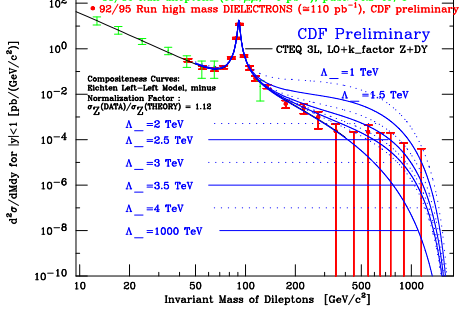

Figure 19: Comparison between CDF Drell-Yan cross-section measurement and the theoretical predictions for various values of the scale $\Lambda_{LL}(qqee)$ (for $\eta = -1$) for the dielectron channel. From ref. [50]

by:

$$\mathcal{L} = \frac{2ie^2}{\Lambda^4} Q_q^2 F^{\mu\sigma} F_\sigma^\nu \bar{q}\gamma_\mu \partial_\nu q \tag{7}$$

where e is the electromagnetic coupling, and Λ is the associated mass scale. The observation of the signatures associated with this operator would be a clear signal of compositeness. Rizzo analyzed the effects of a $q\bar{q} \to \gamma\gamma$ contact interaction at hadron colliders [53]. Fig. 20 shows the integrated event rates for isolated diphoton events with invariant mass larger than $M_{\gamma\gamma}^{min}$ at the LHC with 100 fb^{-1} luminosity. The cross section is changed most at high $M_{\gamma\gamma}^{min}$. In addition the photon pair will tend to be more central with higher average values of p_T. The limits that can be obtained at various hadron colliders are given in Table III. The results show that for a given center of mass energy the $p\bar{p}$ colliders probe higher mass scales than pp colliders because of the higher $q\bar{q}$ luminosity.

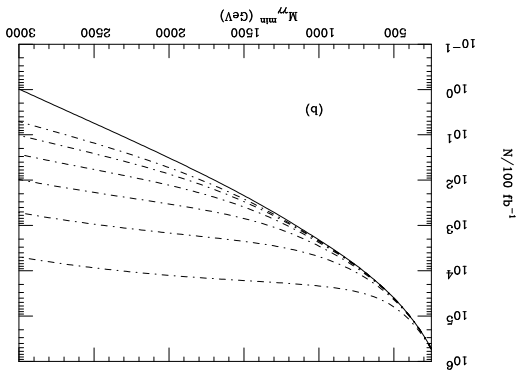

Figure 20: Diphoton pair event rate for the LHC with 100 fb^{-1} as a function of $M_{\gamma\gamma}^{min}$ subject to the cuts $p_t^\gamma > 200$ GeV and $|\eta_\gamma| < 1$. From top to bottom the dash-dot curves correspond to $\Lambda_+ = 0.75$, 1.0, 1.25, 1.75, and 2.0 TeV. The solid curve is the QCD prediction.

The lowest order interactions between a quark and gauge boson are dimension 4 and 5 operators of the form

$$\mathcal{L}_{eff} = g_s \bar{q} T^a \left[-\gamma^\mu G_\mu^a + \frac{\kappa}{4m_q} \sigma^{\mu\nu} G_{\mu\nu}^a - \frac{i\tilde{\kappa}}{4m_q} \sigma^{\mu\nu}\gamma^5 G_{\mu\nu}^a \right] q. \tag{8}$$

This particular case corresponds to interactions between a quark and gluon where $\kappa/2m_q$ and $\tilde{\kappa}/2m_q$ correspond to chromomagnetic (CMDM) and chromoelectric (CEDM) dipole moment couplings of quarks. There are analogous expressions for couplings to the γ and Z. Although these couplings are zero at tree level, within the SM they can be induced at loop level. A related example would be $b \to s\gamma$. One should be cautioned that although the factors in the denominator are taken by convention to be m_q so that these terms may be expressed as quark dipole moments, strictly speaking, Λ, the scale characteristic of substructure or other new physics should be used. These dipole moment couplings are important because they are only suppressed by one power of Λ and also because a nonzero value of the CEDM is a clean signal for CP violation. The above Lagrangian is valid for both light and heavy quarks. In addition to describing an effective qqg vertex it also induces a $qqgg$ interaction which is absent in the SM.

Cheung and Silverman studied the effects of anomalous CMDM and CEDM of light quarks on prompt photon production [54]. Prompt photon production is sensitive to the gluon luminosity inside a hadron because it is mainly produced by quark-gluon scattering. For the same reason it is also sensitive to anomalous couplings of quarks to gluons. The contributing subprocesses for prompt photon production are $q(\bar{q})g \to \gamma q(\bar{q})$ and $q\bar{q} \to \gamma g$. The prompt photon p_T spectrum is shown in Fig. 21 for the SM and for nonzero values of κ. Nonzero values of κ increases the cross section in the high $p_T(\gamma)$ region. They found that CDF and D0 data excludes $\kappa' = \kappa/2m_q < 0.0045$ GeV^{-1}. However, as stated above, if we rescale κ' with a value of $\Lambda = 1$ TeV we find $\kappa < 4.5$. Naively, we would expect $\kappa \sim \mathcal{O}(1)$. Silverman and Cheung further estimated the sensitivity of the Tevatron and LHC to anomalous CMDM's of light quarks. By binning the jet E_T distributions such that each bin would have at most a 10% statistical error from SM QCD they obtained the sensitivities to $\kappa' \equiv 1/\Lambda$ given in Table III [55]. Note that these sensitivities are based on $1-\sigma$ or 68% CL. The effects due to nonzero CEDM will be the same because the increase in cross section is proportional to $(\kappa^2 + \tilde{\kappa}^2)$.

Because of the top quark's large mass it is believed by many that the detailed physics of the top quark may be significantly different than the SM and that the top quark may provide a window into physics beyond the SM. Rizzo examined anomalous top quark couplings to gluons via top quark production at hadron colliders [56] and e^+e^- colliders [57]. At hadron colliders the contributing subprocesses to top pair production are $q\bar{q},\ gg \to t\bar{t}$. The existence of a nonzero CMDM will change both the total and differential cross sections. The higher center-of-mass energies at the LHC will probe beyond the top-pair threshold which will result in much higher sensitivities to the CMDM. $d\sigma/dM_{tt}$ and $d\sigma/dp_T$ distributions are shown for the

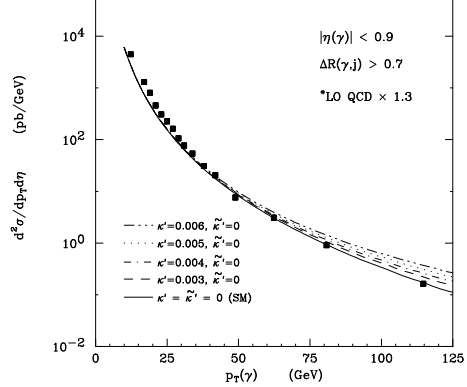

Figure 21: $d^2\sigma/dp_T d\eta$ in prompt γ production for pure QCD and nonzero values of CMDM of quarks. The data points are from CDF. (From Ref. [54].)

SM and with anomalous couplings in Fig. 22 for LHC energies. Non-zero κ leads to enhanced cross sections at large p_T and M_{tt}. Rizzo estimated the sensitivities of these distributions to anomalous couplings using a Monte Carlo approach and taking into account systematic errors. The 95% CL for κ of the top quark are $-0.09 \leq \kappa \leq 0.10$ and $|\kappa| \leq 0.06$ for the M_{tt} and p_t distributions respectively.

Rizzo examined the use of final state gluons as a probe for studying anomalous top-quark couplings at the NLC [57]. He found that the rate and corresponding gluon jet energy distribution for the $e^+e^- \to t\bar{t}g$ are sensitive to the presence of anomalous couplings of the top to the photon and Z at the production vertex as well as to the gluon itself. The sensitivity to anomalous gluon couplings is illustrated in Fig. 23 for a 1 TeV NLC. The resulting constraints are quite complementary to those obtained using other techniques.

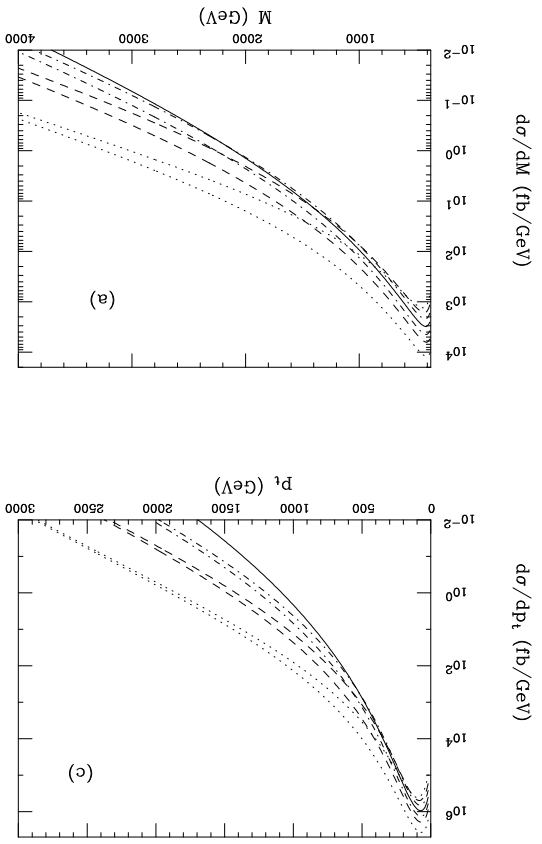

Figure 22: (a) $t\bar{t}$ invariant mass distribution at the LHC for various values of κ assuming $m_t = 180$ GeV. (c) $t\bar{t}$ p_t distribution at the LHC. In all cases, the SM is represented by the solid curve and the upper(lower) pairs of dotted (dashed, dash-dotted) curves correspond to $\kappa = 0.5$ (-0.5), 0.25 (-0.25), 0.125 (-0.125) respectively. From ref. [56]

3. *Excited Fermions*

Although it is expected that the first evidence for quark and/or lepton structure would arise from the effects of contact interactions direct evidence would be given by the observation of excited fermions. Harris investigated the prospects for discovering an excited quark u^* or d^* decaying to dijets at hadron colliders [58]. The qgq^* interaction is described by

$$\mathcal{L}_{eff} = \frac{g}{2\Lambda}\bar{Q}\sigma^{\mu\nu}G_{\mu\nu}q \qquad (9)$$

where Q represents the excited quark. Harris considered the process $qg \to q^* \to qg$ via a dijet resonance signal and included QCD background assuming an experimental dijet mass resolution of 10%. The estimated 5σ discovery mass reach is 1.1 TeV at TeV33, 6.3 TeV at the LHC, 25 TeV at a 50 TeV pp collider, and 78 TeV at the 200 TeV PIPETRON collider.

V. FINAL THOUGHTS

In this report we examined the potential of future collider facilities to study a broad range of new phenomena. The range of physics topics that we examined covered specific cases of new phenomena such as new gauge bosons, new fermions, and difermions, to more subtle hints of physics beyond the standard model via low energy effective operators which subsume the effects of new physics at a much higher energy scale. To deal with this abundance of possibilities, it seems to us that the most prudent approach in deciding upon future facilities is to ensure that we are prepared for all of these possibilities. We should have the capability to explore as many examples of new physics as our imagination can conceive and in as many processes as we can. The ideal situation for this is to have hadron and lepton collider facilities with comparable constituent center of mass energies. As likely as not, when nature finally reveals her mysteries it will be totally unexpected.

At the time of writing, the two HERA experiments have indicated an unexpected excess of events in Deep Inelastic Scattering at high Q^2. To interpret these observations (assuming they are not due to a statistical fluctuation), results from a broad

Table III: New Interactions search reaches in TeV.

Interaction	TeV	TeV33	LHC	pp	NLC	NLC	NLC	NLC	$\mu^+\mu^-$	$\mu^+\mu^-$
$\sqrt{s}$ (TeV)	2	2	14	200	0.5	1.0	1.5	5.0	0.5	4.0
L fb^{-1}	0.11	30	100		50	200	200	1000	50	1000
Dimension 5 Anomalous Couplings										
Λ	2.8	3.5	17		~ 5	~ 10				
Dimension 6 4-fermion Contact Interactions										
$\Lambda_{LL}(ee \to \mu\mu)$	—	—	—	—	32	63	77	210	28	170
$\Lambda_{LR}(ee \to \mu\mu)$	—	—	—	—	29	57	70	190	25	150
$\Lambda_{RL}(ee \to \mu\mu)$	—	—	—	—	29	58	70	190	25	150
$\Lambda_{RR}(ee \to \mu\mu)$	—	—	—	—	31	62	76	210	27	160
$\Lambda_{LL}(q\bar{q} \to \ell\ell)$	2.9	14	—	—						
$\Lambda_{LL}(q\bar{q} \to q\bar{q})$	1.6	—	15	—						
$\Lambda_{LL}(ee \to c\bar{c})$	—	—	—	—	33	65	80	210	19	110
$\Lambda_{LR}(ee \to c\bar{c})$	—	—	—	—	28	57	69	190	16	92
$\Lambda_{RL}(ee \to c\bar{c})$	—	—	—	—	27	49	60	160	5.7	42
$\Lambda_{RR}(ee \to c\bar{c})$	—	—	—	—	34	62	76	210	15	90
$\Lambda_{LL}(ee \to b\bar{b})$	—	—	—	—	38	75	92	250	29	180
$\Lambda_{LR}(ee \to b\bar{b})$	—	—	—	—	30	61	77	210	22	140
$\Lambda_{RL}(ee \to b\bar{b})$	—	—	—	—	33	65	78	230	21	120
$\Lambda_{RR}(ee \to b\bar{b})$	—	—	—	—	33	67	82	250	20	120
Dimension 8 Contact Interactions										
$\Lambda^+(q\bar{q} \to \gamma\gamma)$	0.75	—	2.8	23						
$\Lambda^-(q\bar{q} \to \gamma\gamma)$	0.71	—	2.9	16						
Discovery Reach for Excited Quarks										
	0.75	1.1	6.3	78	—	—	—	—	—	—

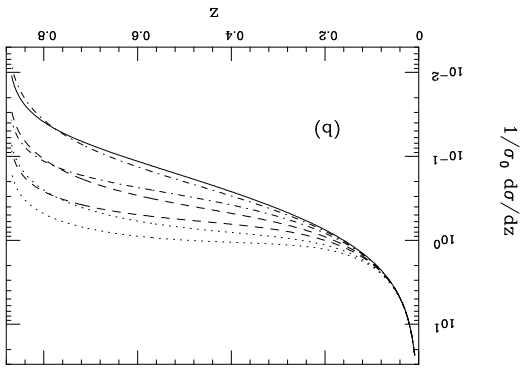

Figure 23: Gluon jet energy spectrum assuming $\alpha_s = 0.10$ for $m_t = 175$ GeV at $\sqrt{s} = 1$ TeV. The upper (lower) dotted, dashed, and dot-dashed curves correspond to κ values of 3(-3), 2(-2), and 1(-1) respectively while the solid curve is conventional QCD with $\kappa = 0$. From ref. [57]

range of experiments have been found to be important: from the low energy precision atomic parity violation measurements to high energy results at the 1.8 TeV Tevatron $p\bar{p}$ collider and the 200 GeV LEP II e^+e^- collider. This is a critical lesson; that although new physics may make its appearance at one facility, eg, the LHC, it is highly likely that measurements at a complementary facility such as the NLC may be crucial to understanding its significance, or visa versa. To have the best chance of discovering and understanding physics beyond the standard model requires a diversified program of new facilities.

VI. ACKNOWLEDGEMENTS

S.G., J.H., and L.P. would like to thank the new phenomena working group members and subgroup leaders for their enthusiasm and hard work. The authors also thank Robert Harris, Mathew Jones, and Tom Rizzo for their special assistance in the completion of this manuscript. This work is supported in part by the U.S. Department of Energy under contracts DE-AC03-76SF00515 and W-31-109-ENG-38, and the Natural Sciences and Engineering Research Council of Canada.

VII. REFERENCES

[1] *Proceedings of the 1982 DPF Summer Study on Elementary Particle Physics and Future Facilities*, Snowmass, CO, 1982.

[2] For a review and original references, see, J.L. Hewett, T. Takeuchi, and S. Thomas, to appear in *Electroweak Symmetry Breaking and Physics Beyond the Standard Model*, ed. T. Barklow *et al.*, (World Scientific, Singapore).

[3] J.L. Hewett, Phys. Rev. Lett. **70**, 1045 (1993); V. Barger, M. Berger, and R.J.N. Phillips, Phys. Rev. Lett. **70**, 1368 (1993); M.S. Alam *et al.*, (CLEO Collaboration), Phys. Rev. Lett. **74**, 2885 (1995).

[4] G. Altarelli and R. Rückl, Phys. Lett. **B259**, 357 (1991); J. Ellis and S. Rudaz, Phys. Lett. **B260**, 447 (1991).

[5] U. Amaldi *et al.*, Phys. Lett. **B281**, 374 (1992).

[6] N.G. Deshpande, E. Keith, and T.G. Rizzo, Phys. Rev. Lett. **70**, 3189 (1993).

[7] T.G. Rizzo, Phys. Rev. **D45**, 3903 (1992); H. Murayama and T. Yanagida, Mod. Phys. Lett. **A7**, 147 (1992); U. Amaldi *et al.*, Phys. Lett. **B281**, 374 (1992).

[8] J.L. Hewett and T.G. Rizzo, [hep-ph/9703337].

[9] M. Cvetic and S. Godfrey, to be published in *Electroweak Symmetry Breaking and Physics Beyond the Standard Model*, eds. T. Barklow, S. Dawson, H. Haber, and J. Seigrist (World Scientific, 1996) [hep-ph/9504216].

[10] T. Rizzo, these proceedings [hep-ph/9612440].

[11] J. D. Lykken, these proceedings [hep-ph/9610218].

[12] D. Toback, these proceedings.

[13] S. Godfrey, Phys. Rev. **D51**, 1402 (1995).

[14] T. Rizzo, these proceedings [hep-ph/9609248].

[15] S. Capstick and S. Godfrey, Phys. Rev. **D37**, 2466 (1988).

[16] C.-E. Wulz, these proceedings.

[17] S. Godfrey, these proceedings [hep-ph/9612384].

[18] F. Cuypers, these proceedings [hep-ph/9611336]; see also F. Cuypers, Nucl. Phys. **B474**, 72 (1996) [hep-ph/9602426].

[19] S. Riemann, these proceedings [hep-ph/9610513]; see also A. Leike and S. Riemann, Appears in *Proceedings of Physics with e^+e^- Linear Colliders Workshop*, Annecy – Grand Sasso – Hamburg 1995, ed. P. Zerwas [hep-ph/9604321]; A. Leike, Z. Phys. **C62**, 265 (1994).

[20] J. Hewett, these proceedings.

[21] A. Djouadi, J. Ng and T.G. Rizzo, to appear in *Electroweak Symmetry Breaking and Physics Beyond the Standard Model*, ed. T. Barklow *et al.*, (World Scientific, Singapore).

[22] M.S. Berger and W. Merritt, these proceedings [hep-ph/9611386].

[23] J.L Hewett and T.G. Rizzo, Phys. Rep. **183**, 193 (1989).

[24] C. Adloff *et al.*, (H1 Collaboration), DESY Report 97-24; J. Breitweg *et al.*, (ZEUS Collaboration), Desy Report 97-25.

[25] W. Buchmüller, R. Rückl and D. Wyler, Phys. Lett. **B191**, 442 (1987).

[26] F. Cuypers and S. Davidson, these proceedings, [hep-ph/9609487].

[27] T.G. Rizzo, these proceedings, [hep-ph/9609267].

[28] G. Wrochna, these proceedings.

[29] M.A. Doncheski and S. Godfrey, these proceedings [hep-ph/9612385].

[30] M.S. Berger, these proceedings [hep-ph/9609517].

[31] P. Kalyniak and I. Melo, these proceedings [hep-ph/9612315].

[32] T.G. Rizzo, Phys. Lett. **116B**, 23 (1982) and Phys. Rev. **D50**, 5602 (1994); D. London, G. Belanger and J.N. Ng, Phys. Lett. **188B**, 155 (1987).

[33] C. Heusch, these proceedings.

[34] C. Greub and P. Minkowski, these proceedings.

of the TeV-2000 Study Group, ed. D. Amidei and R. Brock, Fermilab-Pub-96.082 (1996).

[36] Report of the working group on the strongly interacting weak sector, these proceedings, T. Barklow *et al.*.

[37] K. Cheung and R. Harris, these proceedings [hep-ph/9610382].

[38] E. Eichten and K. Lane, these proceedings [hep-ph/9609297].

[39] D. Toback, these proceedings, Fermilab-Conf-96/360.

[40] J. Womersley, these proceedings, Fermilab-Conf-96/431.

[41] T. Lee, these proceedings.

[42] C.T. Hill, Phys. Lett. **B345**, 483 (1997); C.T. Hill and S. Parke, Phys. Rev. **D49**, 4454 (1994); G. Burdman, these proceedings; T. Barklow *et al.*, these proceedings.

[43] E. Simmons, these proceedings; and Phys. Rev. **D55**, 1678 (1997).

[44] R.S. Chivukula, and J. Terning, Phys. Lett. **B385**, 209 (1996).

[45] R. Harris, these proceedings [hep-ph/9609318].

[46] W. Buchmüller, Acta Phys. Austriaca Suppl. XXVII, 517 (1985); W. Buchmüller and D. Wyler, Nucl. Phys. **B268**, 621 (1986).

[47] J. Layssac *et al* [hep-ph/9602327].

[48] K. Cheung, S. Godfrey, and J. Hewett, these proceedings [hep-ph/9612257].

[49] K.S. Kumar, these proceedings.

[50] P. de Barbaro *et al.*, these proceedings, Fermilab-Conf-96/356-E.

[51] F. Abe *et al.*, (CDF Collaboration) Fermilab-Pub-96/317-E [hep-ex/9609011].

[52] U.S. ATLAS and U.S. CMS Collaborations, edited by I. Hinchliffe and J. Womersley, LBNL-38997 (1996).

[53] T. Rizzo, Phys. Rev. **D51**, 1064 (1994); T. Rizzo, these proceedings.

[54] K. Cheung and D. Silverman, these proceedings [hep-ph/9609455].

[55] K. Cheung and D. Silverman, these proceedings [hep-ph/9610318].

[56] T. Rizzo, these proceedings [hep-ph/9609311].

[57] T. Rizzo, these proceedings [hep-ph/9610373].

[58] R.M. Harris, these proceedings [hep-ph/9609319].